Nitrogen Dioxide Release in the 302 nm Band Photolysis of Spray-Frozen Aqueous Nitrate Solutions. Atmospheric Implications

Yael Dubowski, A. J. Colussi,* and M. R. Hoffmann*

W. M. Keck Laboratories for Environmental Science, California Institute of Technology, Pasadena, California 91125

Received: November 14, 2000; In Final Form: March 7, 2001

We quantify the NO_2 fluxes released into the gas phase during the continuous $\lambda \sim 300$ nm photolysis of NO_3^- in submillimeter ice layers produced by freezing aqueous KNO_3 sprays on cold surfaces. Fluxes, F_{NO_2}, increase weakly with $[NO_3^-]$ between $5 \leq [NO_3^-]/\text{mM} \leq 50$ and increase markedly with temperature in the range of $268 \geq T/\text{K} \geq 248$. We found that F_{NO_2}, the photostationary *concentration* of NO_2^- (another primary photoproduct), and the *quantum yield* of 2-nitrobenzaldehyde in situ photoisomerization are nearly independent of ice layer thickness d within $80 \leq d/\mu\text{m} \leq 400$. We infer that radiation is uniformly absorbed over the depth of the ice layers, where NO_3^- is photodecomposed into NO_2 (+ OH) and NO_2^- (+ O), but that only the NO_2 produced on the uppermost region is able to escape into the gas phase. The remainder is trapped and further photolyzed into NO. We obtain $\phi_{NO_2^-} \sim 4.8 \times 10^{-3}$ at 263 K, i.e., about the quantum yield of nitrite formation in neutral NO_3^- aqueous solutions, and an apparent quantum yield of NO_2 release $\phi'_{NO_2} \sim 1.3 \times 10^{-3}$ that is about a factor of 5 smaller than solution ϕ_{OH} data extrapolated to 263 K. These results suggest that NO_3^- photolysis in ice takes place in a liquidlike environment and that actual ϕ'_{NO_2} values may depend on the morphology of ice deposits. Present ϕ'_{NO_2} data, in conjunction with snow albedo and absorptivity data, lead to F_{NO_2} values in essential agreement with recent measurements in Antarctic snow under solar illumination.

Introduction

Deposition of inorganic nitrate on ice surfaces is a major sink for atmospheric nitrogen oxides.[1,2] The fact that nitrate concentrations in Antarctic ice, in contrast with other major anions, are remarkably constant across the continent suggest remote, global sources.[3] Therefore, nitrate levels within ice cores would provide, if preserved,[4] valuable paleoatmospheric and paleoclimatic information. However, there is mounting evidence that nitrate is processed and reemitted as NO_x from sunlit snowpacks. Recent experiments reveal the photochemical production of NO and NO_2 in and above surface snow at polar and midlatitude regions.[5−8] The photochemical lability of the nitrate incorporated into cirrus clouds is also relevant to various atmospheric processes regulated by the partitioning between NO_x and NO_y species.

Laboratory studies confirm that ice surfaces can efficiently remove HNO_3 from the gas phase. However, although nitrate photolysis in aqueous solutions has been extensively investigated in the UV-A and UV−B regions,[9−14] the photochemical behavior of nitrate in ice and snow under ambient conditions prevalent at high latitudes remains an open issue. In this paper, we report quantitative data on nitrite formation and NO_2 emissions during the 302 nm band photolysis of nitrate in spray-frozen aqueous solutions as a function of temperature, nitrate concentration (in the mM range), and ice layer thickness. We find that primary quantum yields for NO_2 and NO_2^- production in ice are comparable to solution phase values. However, the photodecomposition of the NO_2 rejected by the solid under dim sunlight competes favorably with NO_2 diffusion in ice over submillimeter lengths, limiting its release into the gas phase. Present results are then used to estimate NO_2 fluxes from illuminated snowpacks. The accord obtained vis-à-vis recent field measurements in Antarctica at 70° S is within experimental uncertainties.[8]

* To whom correspondence should be addressed. Phone: (626) 395-4391. E-mail: mrh@its.caltech.edu.

Experimental Section

The experimental setup is shown in Figure 1a,b. Nitrate-doped ice deposits were prepared by spraying precooled KNO_3 (Fisher Scientific) solutions of variable concentration at pH < 6 on a gold-coated cylindrical coldfinger (CF; Figure 1b; total area $A = 182.2$ cm^2) maintained at 248 K by coolant circulation. The ice-covered CF was then sealed inside a quartz sheath (QS) and the array placed inside a reflective aluminum chamber (Figure 1a). Ice deposits were brought to the desired temperature (268, 263, or 248 K) and then irradiated by three Hg Pen-Ray UV lamps (UVP, modal 90-0001-04), symmetrically located around the QS, emitting at $\lambda = 313 \pm 20$ nm. The stability of the lamp output during the (necessarily) long experiments was monitored with a photocell (UDT Sensors, model PIN UV 100L) attached to the top of the aluminum chamber. The chamber was flushed with dry air to prevent moisture condensation on the outer QS surface.

The photon flux incident onto the QS, $I_i = 9.8 \times 10^{14}$ photons cm^{-2} s^{-1}, was determined from actinometric measurements using a potassium ferrioxalate solution filling the QS at 298 K.[15] The photon flux actually absorbed by nitrate-doped ice I_{a,NO_3^-} was evaluated (see below) from the rates of 2-nitrobenzaldehyde (2-NBA) photoisomerization into 2-nitrosobenzoic acid within the ice layers. The latter were also obtained by spray-freezing a 33 μM aqueous 2-NBA solution, which has an absorbance comparable to nitrate solutions in the relevant spectral range, onto the CF. We assume that the intramolecular

10.1021/jp0042009 CCC: $20.00
Published on Web 04/28/2001

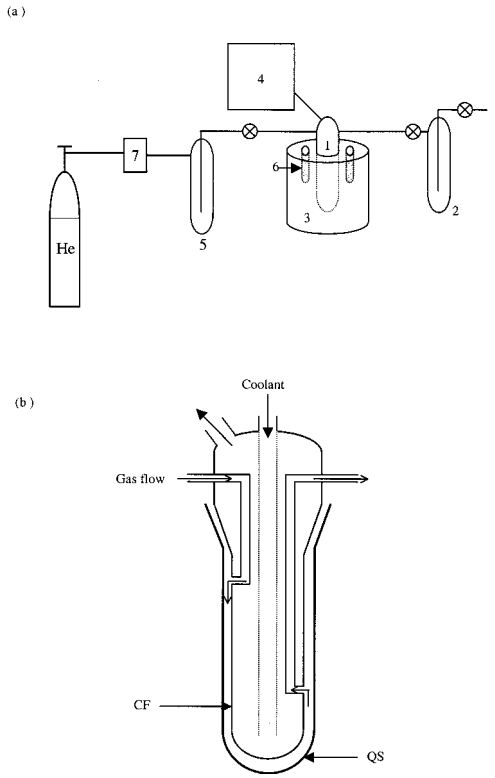

Figure 1. (a) Scheme of the experimental setup. 1. Reaction cell (see Figure 1b); 2. NO_2 condensing trap; 3. Reflective reaction chamber; 4. Circulating cryostat; 5. Molecular sieve at 77 K; 6. Pen-Ray UV lamps nominally emmiting at 313 nm; 7. Flow meter. (b) The reaction cell. CF: Gold coated CF. QS: Quartz sheath.

photoisomerization of 2-NBA in ice, as in all of the phases in which it has been studied, has a quantum yield of $\phi_{iso} = 0.5$, independent of temperature.[16−18] The concentrations of 2-NBA and 2-nitrosobenzoic acid were determined, after thawing, by high-pressure liquid chromatography (HP 1090) with ODS hypersil and Pinnacle IBD columns. The eluent was a 20:80% mixture of methanol and water, and the wavelengths of the detector were set at 235 and 320 nm.

Nitrogen dioxide produced photochemically and released into the gas phase was swept out of the irradiated zone by a steady helium flow (∼10 cm^3 min^{-1}) and condensed downstream into a trap maintained at 77 K, in which 1 cm^3 of a 0.1 M NaOH solution had been previously frozen. The helium (UHP) carrier was prepurified by passage through molecular sieve at 77 K. Experiments were terminated by turning the lamps off and then thawing the ice deposits by raising the temperature of the CF under carrier flow. The condensing trap was then evacuated, sealed, thermalized at 298 K, and kept in the dark for about 12 h to allow any NO_2 present to dissolve into the NaOH solution. The contents of this trap, as well as the melted ice left in the QS, were then analyzed for nitrite using the Saltzmann reagent.[19]

Results and Discussion

The $\lambda > 300$ nm photolysis of nitrate in aerated aqueous solutions at pH < 6 proceeds via two pathways:

$$NO_3^- + H^+ + h\nu \rightarrow NO_2 + OH \quad (1)$$

$$NO_3^- + h\nu \rightarrow NO_2^- + O(^3P) \quad (2)$$

Peroxynitrous acid, ONOOH, the product (not shown) of yet another possible channel at shorter wavelengths, is apparently absent at $\lambda > 300$ nm.[10] The O atoms generated in reaction 2 may react with O_2 ($[O_2]_{water} \sim 0.3$ mM) via reaction 3 or, preferably, with nitrate via reaction 4 at $[NO_3^-] \geq 5$ mM. Nitrite ($\epsilon_{max} = 22.5$ M^{-1} cm^{-1} at 360 nm) will undergo secondary photolysis, reaction 5, and oxidation by OH radicals, reaction 6:

$$O_2 + O(^3P) \rightarrow O_3 \qquad k_3 = 4 \times 10^9\ M^{-1}\ s^{-1} \quad (3)$$

$$NO_3^- + O(^3P) \rightarrow NO_2^- + O_2 \qquad k_4 = 2 \times 10^8\ M^{-1}\ s^{-1} \quad (4)$$

$$NO_2^- + H^+ + h\nu \rightarrow NO + OH \quad (5)$$

$$NO_2^- + OH \rightarrow NO_2 + OH^- \qquad k_6 = 2 \times 10^{10}\ M^{-1}\ s^{-1} \quad (6)$$

The excitation of the NO_3^- $n \rightarrow \pi^*$ band in aqueous media, that has a maximum decadic absorption coefficient of $\epsilon_{NO_3^-} = 7.5$ M^{-1} cm^{-1} at 305 nm, leads to the formation of OH and $O(^3P)$ in relatively low quantum yields: $\phi_1 \sim 9 \times 10^{-3}$, $\phi_1/\phi_2 \sim 9$. ϕ_1 increases at shorter and longer wavelengths within the $n \rightarrow \pi^*$ band and increases by a factor of 2.2 between 273 and 308 K.[14]

When aqueous solutions are frozen, solutes are largely segregated from the ice phase.[20] Spray-freezing involves the rapid cooling of solution microdroplets upon contact with a borosilicate surface at 248 K. Each frozen droplet, covered by the rejected solute, provides the substrate on which new droplets freeze in turn. Thus, the solute is microscopically, rather than molecularly, dispersed in the ice at the grain boundaries or interstitial pores. These conditions are considered to emulate the microscopic and mesoscopic solute environments in snow deposits and cirrus clouds. The ice−air interface, such as the surface lining the interstitial pores, is known to be covered by a quasiliquid layer whose thickness d varies, for example, between ca. 40 nm at 268 K and ca. 15 nm at 248 K in ice produced by freezing 10 mM KCl solutions.[21] Therefore, upon spray-freezing mM KNO_3 solutions into ice particles larger than a few micrometers, the solute accumulated in the liquid film will exceed the eutectic concentration: $[KNO_3] \sim 1$ M ($T_{eutectic} = 270.2$ K).[22] These considerations suggest that the photolysis of NO_3^- in spray-frozen ice will largely take place in a liquidlike film and, by analogy with liquid-phase experiments, will generate NO_2 and NO_2^- as primary photochemical products with local quantum yields of the order of 1%. Actual quantum yields will be ultimately determined by the extent of light penetration into the medium, and by the probability of NO_2 escaping from the ice network.

We probed light transmission through the ice layers by means of the in situ photoisomerization of 2-nitrobenzaldehyde into 2-nitrosobenzoic acid, an intramolecular process whose quantum yield is phase-independent.[16−18] We found that photoisomerization rates in spray-frozen 33 μM 2-NBA solutions, as determined from the yields of 2-nitrosobenzoic acid in the melt, are independent of d, confirming uniform rates of light absorption across the deposits depth. Limited light penetration would have led to smaller isomerization quantum yields in the thicker layers. The same observation applies to the stationary nitrite concentrations reached in the photolysis of 10 mM KNO_3 spray-frozen solutions at 263 K (Figure 2). The evolution of $[NO_2^-]$ in the photolysis of NO_3^- is given by

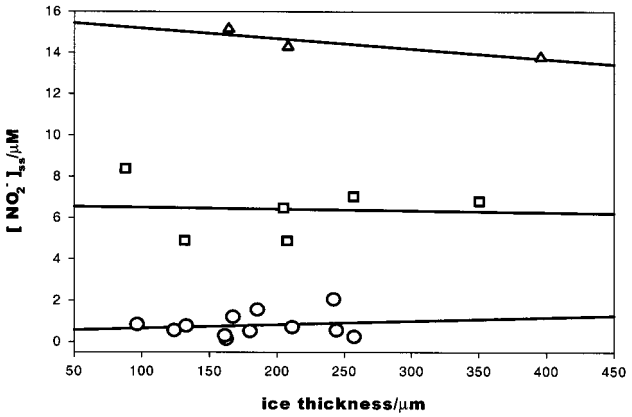

Figure 2. Photostationary nitrite concentrations $[NO_2^-]_{ss}$ as a function of ice layer thickness d at different nitrate concentrations $[NO_3^-]$/mM: 0 (open circles), 10 (open squares), and 50 (open triangles). $T = 263$ K. Solid lines are linear fits. $[NO_2^-]_{ss}$ is considered to be independent of d within the experimental error.

$$\frac{d[NO_2^-]}{dt} = \phi_2 I_{a,NO_3^-} - \phi_5 I_{a,NO_2^-} - k_6[OH]_{ss}[NO_2^-] = \phi_2 I_{a,NO_3^-} - k_{decay}[NO_2^-] \quad (7)$$

where the I_a's are the absorbed photon rates (in photons cm^{-3} s^{-1}) the ϕ's are the corresponding quantum yields, and $[OH^-]_{ss}$ is the rapidly attained steady-state OH radical concentration during the photolysis. Because $I_{a,NO_2^-} \propto [NO_2^-]$, integration of eq 7 leads to

$$[NO_2^-] = \frac{a}{b}[1 - \exp(-bt)] \quad (8)$$

where $a/b = \phi_2 I_{a,NO_3^-}/k_{decay}$ and $b = k_{decay}$. A fit to the $[NO_2^-]$ vs time data in the photolysis of $[NO_3^-] = 10$ mM at 263 K (Figure 3) yields $a = 3.9 \times 10^{-10}$ M s^{-1} and $b = 5.3 \times 10^{-5}$ s^{-1}. Therefore, an estimate of $I_{a,NO3-}$ will provide a ϕ_2 value. As mentioned before, $I_{a,NO3^-}$ can be calculated from 2-NBA in situ photoisomerization rates. The increase of 2-nitrosobenzoic acid concentration with irradiation time indicated that a frozen 33 μM 2-NBA solution absorbs $(7 \pm 1) \times 10^{16}$ photons L^{-1} s^{-1}. To calculate $I_{a,NO3-}$ from this result, it is necessary to evaluate the average extinction coefficients $\langle \epsilon_i \rangle$ of the various species over the lamps output spectrum:[23]

$$\langle \epsilon_i \rangle = \frac{\int_{295nm}^{335nm} \epsilon_{i,\lambda} I_{lamp}(\lambda)\, d\lambda}{\int_{295nm}^{335nm} I_{lamp}(\lambda)\, d\lambda} \quad (9)$$

where $I_{lamp}(\lambda)$ is the lamp emission intensity at λ and $\epsilon_{i,\lambda}$ is the absorption coefficient of species i at λ. We find that $\langle \epsilon_{NO_3^-} \rangle = 2.2$ M^{-1} cm^{-1} and $\langle \epsilon_{2-NBA} \rangle = 976$ M^{-1} cm^{-1}. Hence, from

$$\frac{I_{a,NO_3^-}}{I_{a,2-NBA}} = \frac{\langle \epsilon_{NO_3^-} \rangle}{\langle \epsilon_{2-NBA} \rangle} \frac{[NO_3^-]}{[2-NBA]} \quad (10)$$

we obtain $I_{a,NO_3^-} = (4.9 \pm 1.1) \times 10^{16}$ photons L^{-1} s^{-1} for $[NO_3^-] = 10$ mM. Therefore, $\phi_2 = \phi_{NO_2^-} = a/I_{a,NO_3^-} = (4.8 \pm 1.5) \times 10^{-3}$. This value is within a factor of 2 of the previously reported quantum yields of nitrite formation in the $\lambda > 300$ nm photolysis of aqueous nitrate solutions in the presence of radical scavengers at room temperature: $\phi_{NO_2^-} \sim 6 \times 10^{-3}$.[12-14] In Figure 4, we show $[NO_2^-]_{ss}$ as function of $[NO_3^-]$ in photolyses at 268 and 263 K, as well as in a dark experiment, in the presence of 10 mM CH_3OH as radical scavenger at 263 K, and in the liquid phase T $\sim$ 285 K. It is apparent that $[NO_2^-]_{ss}$ in the liquid phase at $[NO_3^-] = 10$ mM is about a factor of 2 larger than in ice at 268 K.

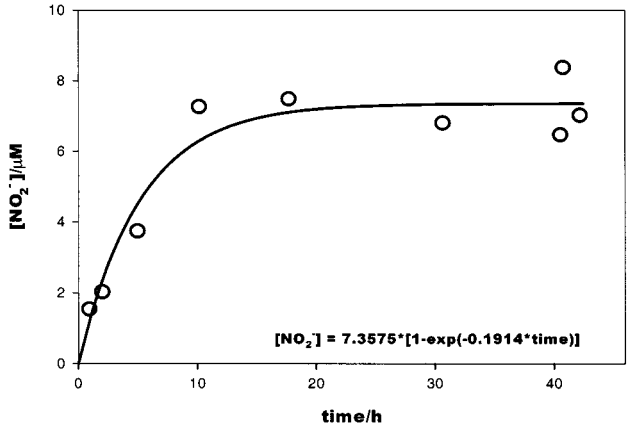

Figure 3. Nitrite concentration as a function of irradiation time. $[NO_3^-] = 10$ mM, 263 K. Open circles are data points. The solid line correspond to $[NO_2^-] = 7.35\,\mu M \times [1 - \exp(-0.19t)]$. Photostationary nitrite concentrations are approached after about 10 h.

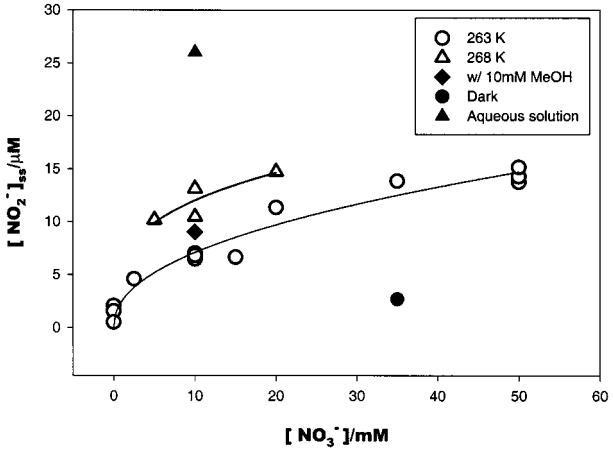

Figure 4. $[NO_2^-]_{ss}$ as a function of $[NO_3^-]$ in nitrate photolyses: in ice at 268 K (open triangles) and 263 K (open circles), in the presence of 10 mM CH_3OH as radical scavenger at 263 K (full diamond), and in the liquid phase at $T \sim 285$ K (full triangle). The full circle is a dark experiment at 263 K.

In contrast with the results of Figure 2 for nitrite, the NO_2 fluxes into the gas phase in the same experiments are nearly independent, or slightly falloff with d (Figure 5). In other words, NO_2 emission rates remain constant despite of the fact that more nitrate is photolyzed in the thicker ice layers. The inevitable conclusion is that only the NO_2 produced in the upper region of the ice deposits is able to escape into the gas phase. Actually, with $\langle \epsilon_{NO_2} \rangle = 210$ M^{-1} cm^{-1}, calculated by means of eq 9 from literature NO_2 absorption cross-sections in the gas phase,[24] secondary photolysis appears to be the main fate of trapped NO_2:

$$NO_2 + h\nu \rightarrow NO + O(^3P) \quad (11)$$

Nitric oxide, the product of reaction 11, is undetectable by our analytical procedures. In Figure 6, we present F_{NO_2} as a function of $[NO_3^-]$ at three ice temperatures, as well as F_{NO_2} data for dark experiments, in the presence of 10 mM CH_3OH, and in the liquid phase. F_{NO_2} from liquid-phase photolysis at 283 K are more than a factor of 3 larger than in ice at 268 K, a result that reflects the competition between the higher NO_2 solubility and faster diffusion in the fluid medium. Because

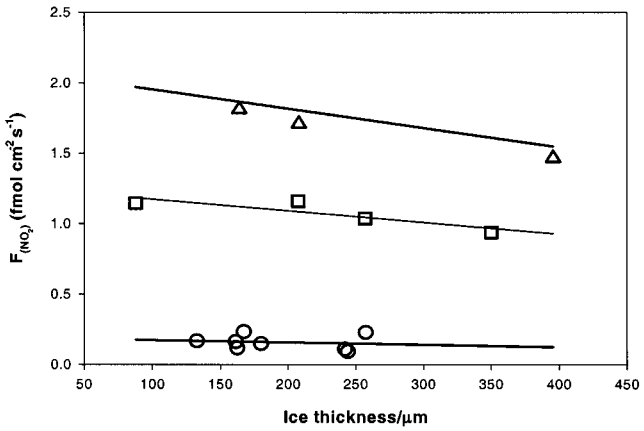

Figure 5. NO_2 flux, F_{NO_2}, as a function of ice thickness d at different $[NO_3^-]$/mM: 0 (open circles), 10 (open squares), and 50 (open triangles). $T = 263$ K. Solid lines are linear fits.

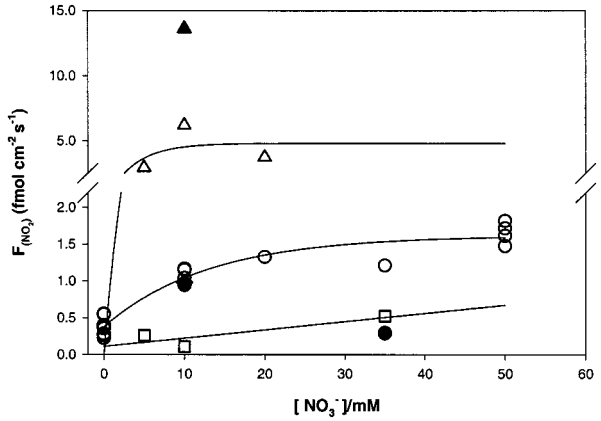

Figure 6. NO_2 flux, F_{NO_2}, as function of $[NO_3^-]$ in photolyses in ice at 268 K (open triangles) and 263 K (open circles), in the presence of 10 mM CH_3OH as radical scavenger at 263 K (full diamond), and in the liquid phase at $T \sim 285$ K (full triangle). The full circle is a dark experiment at 263 K.

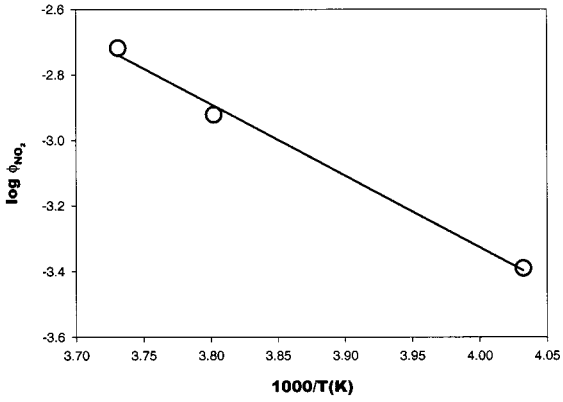

Figure 7. Apparent quantum yield of NO_2 production from irradiation of 10 mM nitrate doped ice as a function of temperature. Average ice thicknesses vary between 125 μm at 268 K, 224 μm at 263 K, and 176 μm at 248 K.

about 40% of the released NO_2 is photolyzed during its residence time ($\tau = 17$ min) in the illuminated zone at typical carrier flow rates, we consider that the actual F_{NO_2} values at the ice surface are a factor of 1.67 larger than determined experimentally. Therefore, we estimate an apparent quantum yield for NO_2 release: $\phi_1' = \phi'_{NO_2} = 1.67\ (F_{NO_2}/d)/I_{a,NO_3^-} = (1.2 \pm 0.9) \times 10^{-3}$ at $[NO_3^-] = 10$ mM, $d \sim 220$ μm, 263 K. However, the primary quantum yield ϕ_1 is expected to be somewhat larger, because F_{NO_2} remains nearly constant down to $d \sim 100$ μm, implying that $\phi_1 > 2.6 \times 10^{-3}$ at $[NO_3^-] = 10$ mM, 263 K.

If one assumes that the thickness of the thinnest ice layer from which 50% of the NO_2 produced photochemically can diffuse into and be detected in the gas phase is about $d_{min} \sim 50$ μm, then it is possible to estimate an effective diffusion coefficient of NO_2 in spray-frozen ice from $D'_{NO_2} = d_{min}^2/(2\tau) \sim (5 \times 10^{-3}\ \text{cm})^2/(2 \times 1275\ \text{s}) = 9.8 \times 10^{-9}\ \text{cm}^2\ \text{s}^{-1}$, and a primary quantum yield of $\phi_1 > 5 \times 10^{-3}$. The latter is in good accord with $\phi_{OH} \sim 5 \times 10^{-3}$ (the value estimated by extrapolation of the data of Zepp's et al. to 263 K),[11] $\phi_{OH} \sim 3 \times 10^{-3}$ (similarly extrapolated from the data of Jankowski et al.),[14] and $\phi_{OH} \sim 7 \times 10^{-3}$ (as measured by Warneck and Wurzinger in the presence of 1 mM scavenger at room temperature).[12] On the other hand, the estimated value of the effective diffusion coefficient D'_{NO_2} is intermediate between $D_{NO_3H} \sim 2 \times 10^{-11}$ $\text{cm}^2\ \text{s}^{-1}$ in bulk ice at 258 K and $D_{NO_3H} \sim 3 \times 10^{-7}\ \text{cm}^2\ \text{s}^{-1}$ on ice surfaces below 253 K.[25−27] The main conclusion is that only the NO_2 produced within ~50 μm of the ice/air interface is actually released into the gas phase.

The temperature dependence of ϕ_1' for $[NO_3^-] = 10$ mM, $d = 200$ μm (Figure 7), is given by

$$\log\phi_1' = 5.42 - \frac{2187}{T} \qquad (12)$$

which should provide a guide to NO_2 fluxes under specific conditions. The stronger temperature dependence of F_{NO_2} relative to nitrite photochemical production (Figure 4) under the same conditions could be ascribed to the enhanced probability of NO_2 escape from the solid and/or the thicker liquid films prevalent at higher temperatures. Further work addressing these issues in underway.

Atmospheric implications

Polar Boundary Layer. Snowpacks are highly reflective disperse materials (effective UV albedo $\beta \sim 0.90-0.95$),[28] that consist of ice microparticles comprising about 40% of the total snow volume. The actinic solar flux penetrating into the snowpacks is partially absorbed by pure ice, and by impurities (e.g., organic matter), leading to overall decadic snow absorptivities $\alpha \sim 5-50\ \text{m}^{-1}$, before being backscattered.[28,29] Nitrate itself present in submicromolar concentrations is a minor chromophore in snowpacks. Therefore, if $\langle J_\lambda \rangle$ is the average solar flux at the surface of the snowpack, the photon flux absorbed by nitrate in a snow column of depth l is given by

$$\langle J_{NO_3^-} \rangle = \langle J_\lambda \rangle (1-10^{-\alpha l}) \frac{\langle \epsilon_{NO_3^-} \rangle [NO_3^-]}{\alpha} \qquad (13)$$

from which the maximum possible NO_2 flux released from the snowpack can be calculated as

$$F_{NO_2} = \phi_1 \langle J_{NO_3^-} \rangle \qquad (14)$$

Jones et al. report $F_{NO_2} = 4.2 \times 10^7$ molecules $\text{cm}^{-2}\ \text{s}^{-1}$ from $l = 20$ cm cubic blocks of natural snow containing $[NO_3^-] = 30$ ng/g $= 0.8$ μM, at 266 K, under a solar irradiance of $\langle J_\lambda \rangle = 30\ \text{W m}^{-2} = 5 \times 10^{15}$ photons ($\langle \lambda \rangle = 337$ nm) $\text{cm}^{-2}\ \text{s}^{-1}$, at the Neumeyer Antarctic station (70° S, 8° W).[8] Assuming $\alpha = 0.15\ \text{cm}^{-1}$ and a snow density of $\delta = 0.4\ \text{g cm}^{-3}$ (i.e., $l = 20\ \text{cm} \times 0.4 = 8$ cm in eq 13), with $\langle \epsilon_{NO_3^-} \rangle = 0.54\ \text{M}^{-1}\ \text{cm}^{-1}$ between 290 and 385 nm (i.e., the spectral interval over which $\langle J_\lambda \rangle$ is measured), we obtain $\langle J_{NO_3^-} \rangle = 1.4 \times 10^{10}$ photons $\text{cm}^{-2}\ \text{s}^{-1}$ and $\phi_1' = 3 \times 10^{-3}$, i.e., within a factor of 2 of the ϕ_1'

value we find for $[NO_3^-] = 10$ mM in ice. The accord is certainly within the uncertainties associated with the assumed properties of snow and the assumed independence of ϕ_1' on $[NO_3^-]$ below 10mM.

Cirrus Clouds. It was suggested recently that the overprediction of the $[HNO_3]/[NO_x]$ ratio in the upper troposphere by current models could be due to the photochemical conversion of HNO_3 into NO_x on ice particles in cirrus clouds.[5] To evaluate this suggestion, we used the quantum yield measured in the present study to estimate the production rate of NO_2 via this pathway. We calculate a maximum production rate of 48 NO_2 molecules cm^{-3} s^{-1} under optimal conditions, i.e, at constant cirrus cover with a surface area of 2×10^{-4} cm^2 cm^{-3},[30] complete adsorption[31] of the extant 400 pptv HNO_3 concentration at 10 km altitude, 35° N,[32] an actinic flux of $\langle J_\lambda \rangle = 1.6 \times 10^{16}$ photon cm^{-2} s^{-1} over the range 290−380 nm,[24] and $\langle \sigma_{NO_3^-} \rangle = 9 \times 10^{-22}$ cm^2 $molecule^{-1}$. Considering that $[NO_2] \sim 40$ pptv ($[NO_2] = [NO_x] - [NO]$ as measured at 10 km),[32] this flux corresponds to a NO_2 lifetime of 68 days, which is much longer then the actual lifetimes (5−7 days) in the upper troposphere.[31] Thus, the NO_3H/NO_2 recycling via absorption and photolysis on ice particles does not seem to resolve the discrepancy between the predicted and measured $[HNO_3]/[NO_x]$ ratio.

Acknowledgment. We are grateful for research funds provided by the foundation Environmental Now.

References and Notes

(1) Logan, J. A. *J. Geophys. Res.* **1983**, *88*, 10785.
(2) Platt, U. In *Chemistry of Multiphase Atmospheric Systems*; Jaeschke, W., Ed.; Springer-Verlag: New York, 1986.
(3) Mulvaney, R.; Wagenbach, D.; Wolff, E. W. *J. Geophys. Res.* **1998**, *103*, 11021.
(4) Wolff, E. W. In *Ice Cores Studies of Global Biogeochemical Cycles, NATO ASI Series, Ser. I*; Delmas, R. J., Ed.; Springer-Verlag: New York, 1995; Vol. I30, p 195.
(5) Honrath, R. E.; Peterson, M. C.; Guo, S.; Dibb, J. E.; Shepson, P. B.; Campbell, B. *Geophys. Res. Lett.* **1999**, *26*, 695.
(6) Honrath, R. E.; Peterson, M. C.; Dziobak, M. P.; Green, S.; Dibb, J. E.; Arsenault, M. A. *Geophys. Res. Lett.* **2000**, *27*, 2237.
(7) Honrath, R. E.; Guo, S.; Peterson, M. C.; Dziobak, M. P.; Dibb, J. E.; Arsenault, M. A. *J. Geophys. Res.* **2000**, in press.
(8) Jones, A. E.; Weller, R.; Wolff, E. W.; Jacobi, H.-W. *Geophys. Res. Lett.* **2000**, *27*, 345.
(9) Mark, G.; Korth, H. G.; Schuchmann, H. P.; von Sonntag, C. *J. Photochem. Photobiol. A: Chem.* **1996**, *101*, 89.
(10) Mack, J.; Bolton, J. R. *J. Photochem. Photobiol. A: Chem.* **1999**, *128*, 1.
(11) Zepp, R. G.; Hoigne, J.; Bader, H. *Environ. Sci. Technol.* **1987**, *21*, 443.
(12) Warneck, P.; Wurzinger, C. *J. Phys. Chem.* **1988**, *92*, 6278.
(13) Alif, A.; Boula P.; *J. Photochem. Photobiol A: Chem.* **1991**, *59*, 357.
(14) Jankowski, J. J.; Kieber, D. J.; Mopper, K. *Photochem. Photobiol.* **1999**, *70*, 319.
(15) Calvert, J.; Pitts, J. N. *Photochemistry*; Wiley: New York, 1966; p 783.
(16) Pitt, J. N.; Hess, L. D.; Baum, E. J.; Schuck, A.; Wan, J. K. S. *Photochem. Photobiol.* **1965**, *4*, 305.
(17) George, M. V.; Scaiano, J. C. *J. Phys. Chem.* **1980**, *84*, 492.
(18) Filby, G. W.; Gunther, K. *Z. Phys. Chem. Neue Folge* **1981**, *125*, 21.
(19) Saltzman, B. E. *Anal. Chem.* **1954**, *26*, 1949.
(20) Gross, G. W.; Wong, P. M.; Hume's, K.; *J. Chem. Phys.* **1977**, *67*, 5264. (b) Gross, G. W.; Gutjahr, A.; Caylor, K. *J. Phys. (Paris)* **1987**, *48C*, 527. (c) Dash, J. G.; Haiying, F.; Wettlaufer, J. S. *Rep. Prog. Phys.* **1995**, *58*, 115.
(21) Doppenschmidt, A.; Butt, H.-J. *Langmuir* **2000**, *16*, 6709.
(22) Seidel, A. *Solubilities*; Van Nostrand: New York, 1940; Vol. 1, p 833.
(23) The spectrum of the lamps (model 90-0001-04) was provided by the manufacturer (UVP).
(24) DeMore, W. B.; Sander, S. P.; Golden, D. M.; Hampson, R. F.; Kurylo, M. J.; Howard, C. J.; Ravishankara, A. R.; Kolb, C. E.; Molina, M. J. Jet Propulsion Laboratory, publication, 1997, 97-4.
(25) Laird, S. K.; Butty, D. A.; Sommerfeld, R. A. *Geophys. Res. Lett.* **1999**, *26*, 699.
(26) Sommerfeld, R. A.; Knight, C. A.; Laird, S. K. *Geophys. Res. Lett.* **1998**, *25*, 935.
(27) Dominé, F.; Thibert, E. *Geophys. Res. Lett.* **1998**, *25*, 4389.
(28) Perovich, D. K.; Govoni, J. W. *Geophys. Res. Lett.* **1991**, *18*, 1233.
(29) Warren, S. G. *Rev. Geophys. Space Phys.* **1982**, *20*, 67. (b) Mellor, M. *J. Glaciology*. **1977**, *19*, 15.
(30) Toon, O. B. Paper presented at international workshop on modeling heterogeneous chemistry of the lower stratosphere/upper troposphere, Le Bischenberg, Bischoffsheim, France, 1996.
(31) Abbatt, J. P. D. *Geophys. Res. Lett.* **1997**, *24*, 1479. (b) Leu, M.-T.; *Geophys. Res. Lett.* **1988**, 15, 17.
(32) Singh, H. B.; Herlth, D.; Kolyer, R.; Salas, L.; Bradshaw, J. D.; Sandholm, S. T.; Davis, D. D.; Crawford, J.; Kondo, Y.; Koike, M.; Talbot, R.; Gregory, G. L.; Sachse, G. W.; Browell, E.; Blake, D. R.; Rowland, F. S.; Newell, R.; Merrill, J.; Heikes, B.; Liu, S. C.; Crutzen, P. J.; Kanakidou, M. *J. Geophys. Res.* **1996**, *101*, 1793.